Cemal Parlak, Özgür Alver and Ponnadurai Ramasami*

Interaction mechanisms and structural properties of B-, Si-doped C60 fullerenes with 1-formylpiperazine

DOI 10.1515/mgmc-2016-0031
Received July 5, 2016; accepted September 15, 2016; previously published online October 21, 2016

Abstract: Piperazines and fullerene nanocages are versatile compounds. These are discussed in a wide range of academic work, especially in the field of medicine, and considered for various applications by the pharmaceutical industry. In the present research, the potential interaction mechanisms between B-, Si-doped C60 and 1-formylpiperazine (1-fp) were examined within the framework of density functional theory, along with their optimized molecular structures and electronic properties. The calculated binding energies and various other physical and chemical parameters of 1-fp found in this work in comparison with the Si- and B-doped fullerenes suggest that doping of fullerene nanocage leads to a strong interaction mechanism that alters the chemical and electronic properties of the investigated compounds. This finding can be used as a guide for their further applications.

Keywords: DFT; electronic properties; fullerenes; surface interaction.

Introduction

Piperazine and its derivatives have found a vast majority of applications in many fields of science, such as chemistry, and in the pharmaceutical industry (Beyeh et al., 2010; Davies et al., 2010; Long et al., 2010; Hatnapure et al., 2012; Li et al., 2014a). For example, several piperazine derivatives have been used as ligands in the synthesis of different types of complexes and clathrates (Parlak et al., 2009a,b). N-substituted piperazine compounds have been shown to have a very wide range of pharmaceutical properties that range from anticancer, antifungal, and antimicrobial to tuberculoastic activities (Liang et al., 2004; Foks et al., 2005; Jiang and Huang, 2012; Wu et al., 2014; Menezes et al., 2016). Further, 1-fp is often in the center of scientific studies, such as those devoted to the synthesis of some antihypertensives, male antifertility products, receptor antagonists, as well as studies investigating the compounds of dopamine D4 receptor imaging (Dwivedi et al., 1991; Ferrarini et al., 1998; Oh et al., 2004; Takahashi et al., 2006).

Density functional theory (DFT) is widely used for the pre-evaluation of synthesized or designed molecular systems due to its low cost and practical applications (Helgaker et al., 1999; Dheivamalar and Sugi, 2015; Hassani and Tavakol, 2014; Li et al., 2015). DFT method has the advantage of giving some insights before experimental applications to avoid excessive amounts of useless experimental efforts. Since their appearance in 1985, fullerenes have enjoyed great attention as suitable candidates for drug delivery systems (Kroto et al., 1985; Bakry et al., 2007; Singh and Lillard, 2009). They have also been in the search for organic photovoltaic devices because of their excellent electronic properties (Renz et al., 2008). In the current research, DFT is used to determine the possible interaction edges of Si-, B-doped C60 fullerenes with 1-fp molecule, thus enabling us to evaluate the fullerene cage as a possible candidate to carry this potentially important molecule for further applications.

Computational details

In order to find the stable configurations of the investigated systems, structures are typically built and geometry optimizations are completed without applying any geometrical restrictions. For large molecular systems, we often encounter imaginary frequencies at the end of the frequency calculations of the optimized structures. This is an indication of a transition structure and not a global energy minimum on the potential energy surfaces. Therefore, in such cases,

***Corresponding author: Ponnadurai Ramasami,** Computational Chemistry Group, Department of Chemistry, Faculty of Science, University of Mauritius, Réduit 80837, Mauritius; and Visiting Professor, Department of Applied Chemistry, University of Johannesburg, Doomfontein 2028, South Africa, e-mail: p.ramasami@uom.ac.mu; ramchemi@intnet.mu
Cemal Parlak: Department of Physics, Science Faculty, Ege University, Izmir 35100, Turkey
Özgür Alver: Department of Physics, Science Faculty, Anadolu University, Eskisehir 26470, Turkey

the optimization process is repeated until no imaginary frequencies are observed at the end of vibrational frequency calculations of the examined structures. In the current study, calculations were carried out using M062X and B3LYP functionals with the 6-31G(d) basis set in both gas and water solvent media. To perform stability and structural assessments and to understand the adsorption mechanisms, binding energy (E_b), frontier energy gap (E_g), chemical hardness (η), and electrophilicity index (ω) were also calculated. Calculations were performed with Gaussian 09 (Frisch et al., 2009). A pictogram of the optimized molecular systems was created using GaussSum and GaussView programs (O'Boyle et al., 2008; Dennington et al., 2009).

Results and discussion

The conformational and vibrational properties of 1-fp have been reported in a previous study (Keşan and Parlak, 2014). On the basis of previously reported data (Keşan and Parlak, 2014) and on calculated electrostatic potential surface (EPS) (Figure 1), two interaction points, O and NH found more negative on the EPS of 1-fp, were suggested as interaction edges with the doped fullerene systems. As can be clearly seen in Figure 1, the introduction of water as a solvent and optimization media slightly changed the charge distribution, particularly at the interaction edges (O, NH). Clearly, hydrogen bonding has a very important impact on the stability and E_b energies of molecular systems (Li et al., 2014b; Djikaev and Ruckenstein, 2016; Ragavendran and Muthunatesan, 2016). Therefore, water inevitably interacts with ligand and doped fullerene cages, thus leading to changes on the adsorption properties and strength of the binding energies.

Considering these interaction sites, optimized structures were obtained, as shown in Figure 2. Boron and silicon atoms were chosen as the active sites for B- and Si-doped fullerene cages, as reported by Hazrati and Hadipour (2016). Effective physical adsorption or interaction of different types of host and guest molecular systems not only relate to the polarity of interaction sites but also to many other factors, such as molecular dynamics, molecular structure, and optimization conditions (Zolek et al., 2003; Umadevi and Sastry, 2012; Izadyar and Housaindokht, 2016). By checking the only partial charges, it is difficult to know which site is more suitable for interaction. However, based on the conclusions of E_b energies, it can be concluded that the BC59…NH system in the gas phase and in water media is more favorable than the

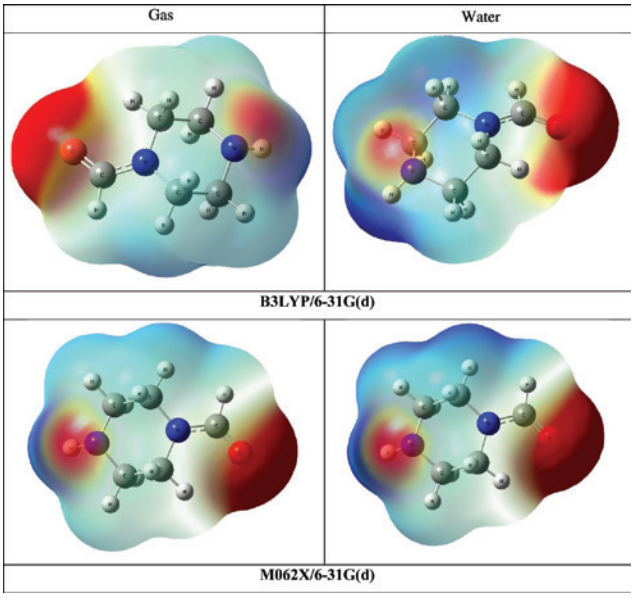

Figure 1: Electrostatic potentials on 1-fp.
Surfaces are defined by the 0.0004 electrons/b^3 contour of the electronic density. Color ranges, in a.u.: blue: more positive than 0.032 and red: more negative than −0.032.

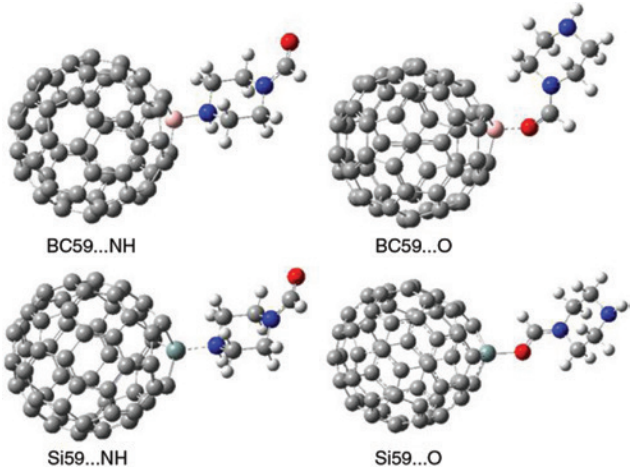

Figure 2: Optimized molecular structures for the investigated systems by M062X/6-31G(d) in the gas phase.

Table 1: Binding and solvent energies (kcal/mol) of the investigated systems.

Structure	M062X/6-31G(d)			B3LYP/6-31G(d)		
	E_b (gas)	E_b (water)	E_{Solv}	E_b (gas)	E_b (water)	E_{Solv}
BC59…NH	−40.74	−45.74	−12.39	−27.17	−31.95	−12.05
BC59…O	−22.94	−26,51	−10.95	−21.17	−24.51	−10.62
SiC59…NH	−41.25	−51.55	−18.01	−26.41	−37.13	−18.03
SiC59…O	−41.79	−51.04	−16.97	−29.89	−39.02	−16.43

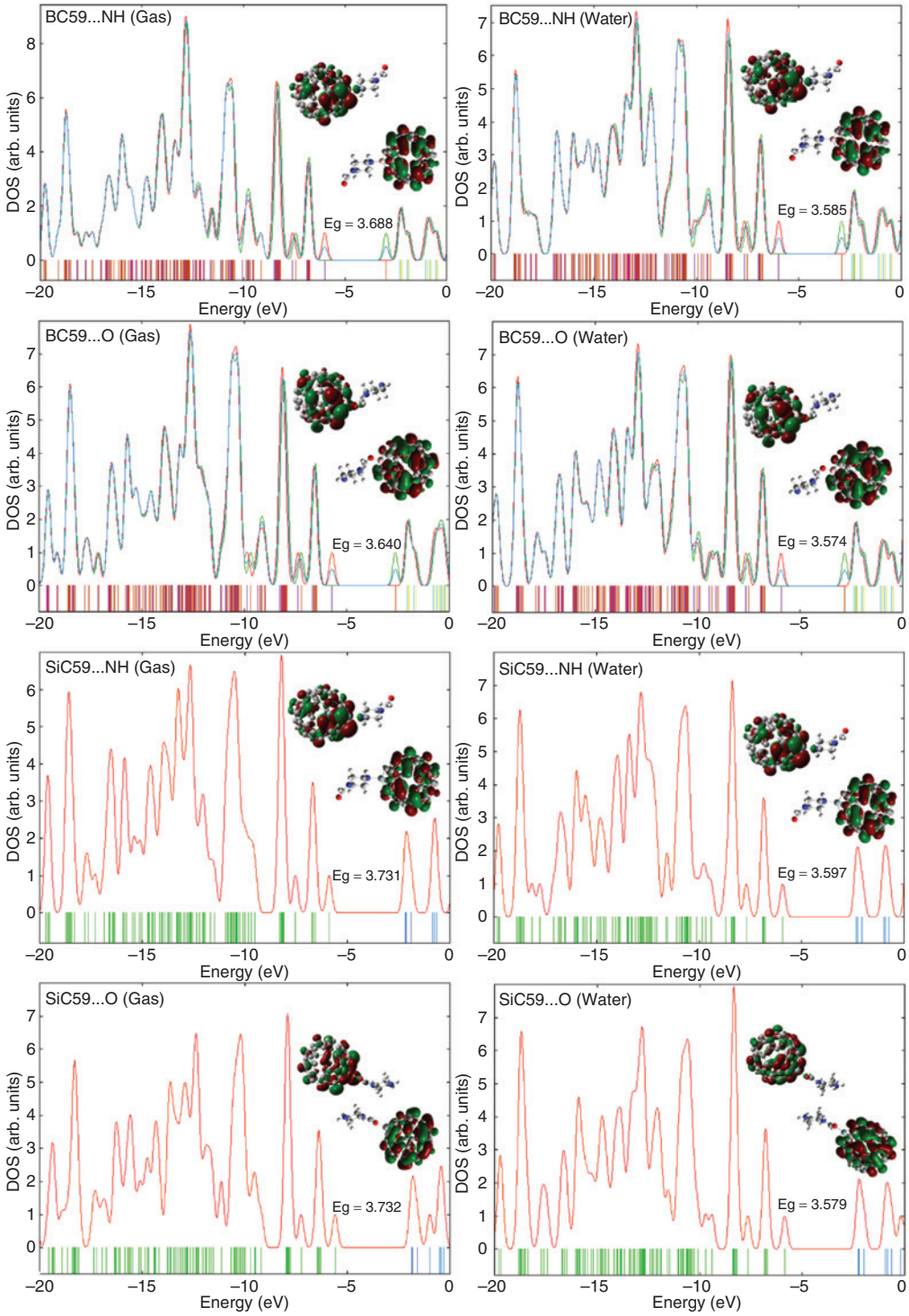

Figure 3: DOS spectra of the investigated structures by M062X/6-31G(d).

BC59…O system, which is confirmed by the calculations of both the M062X and B3LYP functionals. This fact suggests that BC59 and NH of ligand molecule seem to interact more efficiently or boron of C59 can more easily reach and interact with NH than BC59 and O, considering the previously mentioned factors.

The binding and solvent energies (E_b, E_{solv}) calculated by B3LYP/6-31G(d) and M062X/6-31G(d) methods in both the gas phase and water environment are given in Table 1. Silicon and boron have different chemical properties. For example, doping with silicon does not cause a change in the net occupancy of the energy level

Table 2: Some energetic parameters (eV) of the investigated structures.

Structure	HOMO	LUMO	Gap	Chemical hardness	Electrophilicity index
M062X/6-31G(d)					
Gas					
BC59…O	−5.714	−2.074	3.640	1.820	4.166
BC59…NH	−5.995	−2.307	3.688	1.844	4.672
SiC59…O	−5.597	−1.865	3.732	1.866	3.730
SiC59…NH	−5.885	−2.154	3.731	1.866	4.330
Water					
BC59…O	−5.937	−2.363	3.574	1.787	4.819
BC59…NH	−5.979	−2.394	3.585	1.793	4.889
SiC59…O	−5.858	−2.279	3.579	1.790	4.625
SiC59…NH	−5.924	−2.327	3.597	1.790	4.732
B3LYP/6-31G(d)					
Gas					
BC59…O	−4.671	−2.562	2.109	1.055	6.202
BC59…NH	−4.921	−2.833	2.088	1.044	7.199
SiC59…O	−4.493	−2.391	2.102	1.051	5.636
SiC59…NH	−4.775	−2.672	2.103	1.052	6.593
Water					
BC59…O	−4.890	−2.866	2.024	1.012	7.430
BC59…NH	−4.894	−2.896	1.998	0.999	7.593
SiC59…O	−4.749	−2.779	1.970	0.985	7.192
SiC59…NH	−4.801	−2.821	1.980	0.990	7.335

Table 3: Some optimized distances (Å).

Length	M062X	B3LYP	M062X	B3LYP
		Gas		Water
B…NH	1.63	1.66	1.62	1.64
B…O	1.60	1.60	1.56	1.56
Si…NH	1.92	1.95	1.88	1.92
Si…O	1.80	1.83	1.75	1.76

Table 4: NH and C=O stretching frequencies for the studied complexes.

Structure	NH stretching		C=O stretching	
	Gas	Water	Gas	Water
B3LYP/6-31G(d)				
1-fp	3506	3506	1797	1750
BC59…O	3522	3515	1715	1708
SiC59…O	3526	3520	1709	1719
BC59…NH	3413	3422	1805	1757
SiC59…NH	3398	3407	1808	1760
M062X/6-31G(d)				
1-fp	3551	3546	1850	1797
BC59…O	3557	3547	1750	1733
SiC59…O	3561	3570	1745	1773
BC59…NH	3428	3446	1858	1799
SiC59…NH	3419	3414	1861	1808

compared with boron, because silicon and carbon include the same number of valance electrons (Hazrati and Hadipour, 2016). Furthermore, functionals used in the search for E_b energies have potential effects (Bryantsev et al., 2009) that can lead to some differences in the E_b energies. Considering these E_b energies both in the gas and water phases, the interaction with BC59 with NH edge of 1-fp seems to lead to a more stable configuration than the BC59…O structural system. However, these E_b energies of SiC59…NH and SiC59…O structures are almost the same for both gas and water environments. Compared with the gas phase, all the investigated systems in the water phase have lower or more negative E_b energy (Table 1). Based on the E_{solv} energy, it can be concluded that the solubilities of the BC59…NH and SiC59…NH systems have a higher degree than those of the BC59…O and SiC59…O systems, because they have more negative E_{solv} energies (Table 1). The generally accepted energy range for a chemisorption to occur is known to be 10–100 kcal/mol (Bhushan, 1999). This suggests that, considering the E_b values obtained in this work for the investigated systems, a chemisorption occurs between 1-fp and B-, Si-doped fullerene systems.

As can be followed quantitatively on the density of state (DOS) graphs for B- and Si-doped fullerenes (Figure 3), changing the optimization media from gas

to water and interaction sites from NH to O causes some changes in the E_g energies. However, this change is almost negligible from SiC59…NH (gas) to SiC59…O (gas) with an amount of 0.001 eV.

The calculated data for electrophilicity (ω) for the investigated systems show an increase for the structures calculated with the M062X and B3LYP functionals (Table 2). This means that the electrophilic characters of the structures BC59…O and SiC59…O are lower than the BC59…NH and SiC59…NH systems for both gas and water media. Meanwhile, chemical hardness is a measure of resistance to the charge transfer (Makov, 1995), which is strictly related to the doped atom and solvent media. Thus, this may vary depending on the different dopants used for the studied complexes. Chemical hardness of the SiC59…NH and SiC59…O complexes showed very similar results for M062X and B3LYP functionals in the gas phase and water media calculations (Table 2). Furthermore, chemical hardness of the BC59…NH system is higher than that of the BC59…O system with M062X/6-31G(d) level. However, the opposite of this can be observed with the results calculated at B3LYP/6-31G(d) level. This finding suggests that, unlike the electrophilicity indexes, chemical hardness shows different characteristics based on the employed theoretical level. Moreover, B…NH, B…O, Si…NH and Si…O distances have been reduced owing to changes from gas to water media; hence, the binding energy becomes more negative as expected (Table 3).

Table 4 shows the variations of NH and C=O stretching vibrations before and after the interaction. As can be clearly seen, the interaction of 1-fp with Si-, B-doped cages causes some severe alterations with the vibrational frequencies of interaction edges of NH and C=O as expected. In Table 4, the effects of solvent, dopant atom, and the methods used for calculations on the vibrational frequencies of NH and C=O bands can be clearly observed.

Conclusions

The interaction mechanism of B-, Si-doped C60 fullerenes and 1-fp molecule were investigated based on the quantum mechanical calculations, which used M062X and B3LYP functional with 6-31G(d) basis, set in both gas and water environments. For the most stable configurations, two interaction sites were included with 1-fp labelled with NH and O. The stabilities of the investigated systems showed dependence on the computational methods and the solvent media. For instance, it was observed that structures became more stable in water compared with those in the gas phase. The most stable structure obtained with M062X method was the SiC59…NH structure with a binding energy of –51.55 kcal/mol, which is slightly smaller (more negative) than SiC59…O system with a binding energy of –51.04 kcal/mol. In comparison, the most stable structure suggested by the results of B3LYP method was found to be SiC59…O, with a binding energy of –39.02 kcal/mol.

Acknowledgments: We acknowledge the computing resources provided by Fencluster system in the Science Faculty of Ege University. The authors are also thankful to the anonymous reviewers, whose comments proved useful in revising the manuscript.

References

Bakry, R.; Vallant, R. M.; Najam-ul-Haq, M.; Rainer, M.; Szabo, Z.; Huck, Ch.W.; Bonn, G. K. Medicinal applications of fullerenes. *Int. J. Nanomed.* **2007,** *2*, 639–649.

Beyeh, N. K.; Valkonen, A.; Rissanen, K. Piperazine bridged resorcinarene cages. *Org. Lett.* **2010,** *12,* 1392–1395.

Bhushan, B. Principles and Applications of Tribology. 1st Edition; Wiley-Interscience: Ohio, 1999.

Bryantsev, V. S.; Diallo, M. S.; Van Duin A. C. T.; Goddard III, W. A. Evaluation of B3LYP, X3LYP, and M06-class density functionals for predicting the binding energies of neutral, protonated, and deprotonated water clusters. *J. Chem. Theory Comput.* **2009,** *5*, 1016–1026.

Davies, S.; Wood, D. M.; Smith, G.; Button, J.; Ramsey, J.; Archer, R.; Holt, D. W; Dargan, P. I. Purchasing 'legal highs' on the internet-is there consistency in what you get? *Q. J. Med.* **2010,** *103,* 489–493.

Dennington, R. D.; Keith, T. A.; Millam, J. M. GaussView 5. Semichem Inc.: Shawnee Mission, KS, 2009.

Dheivamalar, S.; Sugi, L. Fullerene solubility–current density relationship in polymer solar cells. *Spectrochim. Acta A* **2015,** *151*, 687–695.

Djikaev, Y. S.; Ruckenstein, E. Recent developments in the theoretical, simulational, and experimental studies of the role of water hydrogen bonding in hydrophobic phenomena. *Adv. Colloid Interface Sci.* **2016,** *235,* 23–45.

Dwivedi, A. K.; Shukla, V. K.; Maikhuri, J. P.; Srivastava, A.; Setty, B. S.; Khanna, N. M. Synthesis of some 1-formyl piperazine derivatives and sulfaselazine analogs as a potential male antifertility agents. *Ind. J. Pharmaceut. Sci.* **1991,** *53*, 170–175.

Ferrarini, P. L.; Mori, C.; Badawneh, M.; Calderoneb, V.; Calzolari, L.; Loffredob, T.; Martinottib, E.; Saccomannia, G. Synthesis of 1,8-naphthyridine derivatives: Potential antihypertensive agents – Part VII. *Eur. J. Med. Chem.* **1998,** *33*, 383–397.

Foks, H.; Janowiec, M; Zwolska, Z; Augustynowicz-Kopec, E. Phosphorus sulfur silicon. *Relat. Elem.* **2005**, *180*, 537–543.

Frisch, M. J.; Trucks, G. W.; Schlegel, H. B.; et al. Gaussian 09. Revision A.1, Gaussian Inc.: Wallingford, CT, 2009.

Hassani, F.; Tavakol, H. A DFT, AIM and NBO study of adsorption and chemical sensing of iodine by S-doped fullerenes. *Sensor Actuat. B-Chem.* **2014,** *196*, 624–630.

Hatnapure, G. D.; Keche, A. P.; Rodge, A. H.; Birajdar, S. S.; Tale, R. H.; Kamble, V. M. Synthesis and biological evaluation of novel piperazine derivatives of flavone as potent anti-inflammatory and antimicrobial agent. *Bioorg. Med. Chem. Lett.* **2012,** *22,* 6385–6390.

Hazrati, M. K.; Hadipour, N. L. Adsorption behavior of 5-fluorouracil on pristine, B-, Si-, and Al-doped C60 fullerenes: A first-principles study. *Phy. Lett. A* **2016,** *380*, 937–941.

Helgaker, T.; Jaszunski, M.; Ruud, K. Ab initio methods for the calculation of NMR shielding and indirect spin–spin coupling constants. *Chem. Rev.* **1999,** *99,* 293–352.

Izadyar, S. M., Housaindokht, M. R. Solvent and spin state effects on molecular structure, IR spectra, binding energies and quantum chemical reactivity indices of deferiprone–ferric complex: DFT study. *Polyhedron*. **2016**, *117*, 623–627.

Jiang, D. H.; Huang, M. Design and synthesis of thieno[3,2-d]pyrimidine derivatives containing a piperazine unit as anticancer agents. *Chem. Reag*. **2012,** *34, 797–799*.

Keşan, G.; Parlak, C. New insights into the conformal stability, influence of hydrogen bonding and vibrational analysis of 2,6- and 3,5-Dihydroxyacetophenone – A comparative study. *Spectrochim. Acta A* **2014,** *118,* 1113–1120.

Kroto, H. W.; Heath, J. R.; Obrien, S. C.; Curl, R. F.; Smalley, R. E. C60: Buckminsterfullerene. *Nature* **1985,** *318*, 162–163.

Li, H.; Moullec, Y. L.; Lu, J.; Chen, J.; Valle Marcos, J. C.; Chen, G. Solubility and energy analysis for CO_2 absorption in piperazine derivatives and their mixtures. *Int. J. Greenh. Gas Control* **2014a,** *31,* 25–32.

Li, H.; Liu, Y.; Yang, Y.; Yang, D.; Sun, J. Influences of hydrogen bonding dynamics on adsorption of ethyl mercaptan onto functionalized activated carbons: a DFT/TDDFT study. *J. Photochem. Photobiol. A*, **2014b,** *291,* 9–15.

Li, X.; Ren, H.; Yang, X.; Song, J. Exploring the chemical bonding, infrared and UV–vis absorption spectra of OH radicals adsorption on the smallest fullerene. *Spectrochim. Acta A* **2015,** *144,* 258–265.

Liang, S.; Liu, C. M.; Jin, Y. S.; He, Q. Q. Synthesis and the antifungal activity of 1-(1H-1,2,4-triazol-1-yl)-2-(2,4-difluorophenyl)-3-[(4-substituted)-piperazine-1-yl]-2-ropanols. *Chin. J. Med. Chem.* **2004,** *14*, 71–75.

Long, J. Z.; Jin, X.; Adibekian, A.; Li, W. W.; Cravatt, B. F. Characterization of tunable piperidine and piperazine carbamates as inhibitors of endocannabinoid hydrolases. *J. Med. Chem.* **2010,** *53,* 1830–1842.

Makov, G. Chemical hardness in density functional theory. *J. Phys. Chem.* **1995,** *99*, 9337-9339.

Menezes, A. C.; Campos, P. M.; Euletério, C.; Simões, S.; Praça, F. S.; Bentley, M. V.; Ascenso, A. Development and characterization of novel 1-(1-naphthyl)piperazine-loaded lipid vesicles for prevention of UV-induced skin inflammation. *Eur. J. Pharm. Biopharm.* **2016,** *104,* 101–109.

O'Boyle, N. M.; Tenderholt, A. L.; Langner, K. M. cclib: A library for package-independent computational chemistry algorithms. *J. Comp. Chem.* **2008,** *29*, 839–845.

Oh, S. J.; Lee, K. C.; Lee, S. Y.; Ryu, E. K.; Saji, H.; Choe, Y. S.; Chi, D. Y.; Kim, S. E.; Lee, J.; Kim, B. T. Synthesis and evaluation of fluorine-substituted 1H-pyrrolo[2,3-b]pyridine derivatives for dopamine D_4 receptor imaging. *Bioorg. Med. Chem.* **2004,** *12,* 5505–5513.

Parlak, C.; Alver, Ö.; Şenyel, M. Vibrational spectroscopic study on some Hofmann type clathrates: M(1-Phenylpiperazine)2Ni(CN)4.2G (M = Ni, Co and Cd; G = aniline). *J. Mol. Struct.* **2009a,** *919,* 41–46.

Parlak, C.; Alver, Ö.; Şenyel, M. Vibrational spectroscopic investigations of Hofmann-T_d type complexes: Ni(1-Phenylpiperazine)2M(CN)4 (M = Cd or Hg). *J. Chem. Soc. Pak.* **2009b,** *31,* 888–893.

Ragavendran, V.; Muthunatesan, S. New insights into the conformal stability, influence of hydrogen bonding and vibrational analysis of 2,6- and 3,5-dihydroxyacetophenone – A comparative study. *J. Mol. Struct.* **2016,** *1125,* 413–425.

Renz, J. A.; Troshin, P. A.; Gobsch, G.; Razumov, V. F.; Hoppe, H. Fullerene solubility–current density relationship in polymer solar cells. *Phys. Status Solidi* (*RRL*) **2008,** *2,* 263–265.

Singh, R.; Lillard, J. W. Nanoparticle-based targeted drug delivery. *Exp. Mol. Pathol.* **2009,** *86,* 215–223.

Takahashi, T.; Sakuraba, A.; Hirohashi, T.; Shibata, T.; Hirose, M.; Haga, Y.; Nonoshita, K.; Kanno, T.; Ito, J.; Iwaasa, H.; et al. Novel potent neuropeptide Y Y5 receptor antagonists: Synthesis and structure–activity relationships of phenylpiperazine derivatives. *Bioorg. Med. Chem.* **2006,** *14,* 7501–7511.

Umadevi, D.; Sastry, G. N. Metal ion binding with carbon nanotubes and graphene: Effect of chirality and curvature. *Chem. Phys. Lett.* **2012,** *549*, 39–43.

Wu, Q.; Wang, Z. C.; Wei, X.; Xue, W. Synthesis and antibacterial activities of 1-substituted-4-[5-(4-substitutedphenyl)-1,3,4-thiadiazol-2-sulfonyl]piperazine derivatives, *Chin. J. Synth. Chem.* **2014,** *22,* 429–434.

Zolek, T.; Paradowska, K.; Wawer, I. ^{13}C CP MAS NMR and GIAO-CHF calculations of coumarins. *Solid State Nucl. Magn. Reson.* **2003,** *23,* 77–87.